**DOE/Office of Science Program**

**Office:** High Energy Physics

**DOE Contact**: Dr. David Boehnlein

301-903-7843 David.

Boehnlein@science.doe.gov

**L. RECIPIENT / CONTRACTOR POINT OF CONTACT**

**Name and/or Position:** Prof. Joseph M. Izen
**E-mail:** joe@utdallas.edu
**Phone:** 972 546 2540
**Organization:** University of Texas at Dallas

## AN 241.3 - Announcement of USDOE Scientific and Technical Information

**(For use by Financial Assistance Recipients and Non-Major Site/Facility Contractors)**

**OSTI ID:** 1096621

**SITE CODE:** CHO - Chicago Operations Office, Argonne, IL (United States)

## Part I: STI PRODUCT DESCRIPTION

**A. STI PRODUCT IDENTIFIERS:**

***1. Report/Product Number(s):** DOE-UTD-41310

***2. DOE Contract Number(s):** FG02-04ER41310

**3. Other Identifying Number(s):**

***B. ORIGINATING RESEARCH ORGANIZATION:** University of Texas at Dallas, Richardson, TX FInal Report: DE-FG02-04ER41310

***C. STI PRODUCT TITLE:** Elementary Particle Physics Grant monitor: David Boehnlein

***D. AUTHOR(s):** Izen, Joseph M., Ishak-Boushaki, Mustapha

**Author E-mail Address(es):**

***E. STI PRODUCT PUBLICATION/ISSUE DATE:** 10/18/2013

**Availability:**

***F. STI PRODUCT TYPE:** Technical/Workshop Report

**Technical Report Type:** Final

**G. STI PRODUCT OR TECHNICAL REPORTING PERIOD** 04/15/2010thru06/30/2013

**H. SPONSORING ORGANIZATION:** USDOE; USDOE Office of Science (SC)

**I. SUBJECT CATEGORIES:** 72 PHYSICS OF ELEMENTARY PARTICLES AND FIELDS

**Keywords:** Elementary Particles LHC ATLAS

**J. DESCRIPTION/ABSTRACT:**

ATLAS and the LHC are delivering on the promise of discovery physics at the high energy frontier. Using 4.8 fb?1 of 2011 √s=7 TeV data and the first 5.8 fb?1 of 2012 √s=8 TeV data, ATLAS published the observation of a new particle with a mass of 126 GeV with a significance of 5.9σ that is compatible with a Standard Model (SM) Higgs. The LHC is outperforming intial projections for the 2012 run, and ATLAS is on track to integrate ~20 fb^(-1) of proton-proton collisions in 2012 before Long Shutdown 1 (LS1) begins in Spring 2013. University of Texas at Dallas (UTD) physicists will complete work on two ATLAS analyses this fall. The first is the search for the gauge bosons of a hypothesized dark sector. For 2011 data, UTD is responsible for the ?dark photon? search in the electron-jet channel, and we are looking forward to an expanded leadership role in the dark photon search using the full 2012 data set. Our second analysis interest is the study of X/Y/Z exotic states having $c\bar{c}$ content, which builds on our experience in this field from the BABAR experiment After completing a measurement of the Xc(3872) production cross section this fall, we will search for evidence of the Z(4430)+ which is reported by Belle but not confirmed by BABAR. The UTD group has played a strong role in ATLAS operations, with group members serving as Pixel Run Coordinator, ATLAS Shift Leader, and Pixel/Inner Detector Shifter. For most of the current 3-year funding cycle, a group member coordinated the development of the Pixel DAQ code, and another continues to build and maintain the data quality monitoring (DQM) application that is used by the Inner Detector control room shifter. Additionally, members of our group take Pixel on-call expert shifts for DQM and DAQ. We led an optoboard lifetime study to assess concerns of premature on-detector VCSEL failure using the Pixel working prototype detector at CERN. Physicists based at UTD participated through Pixel Offline DQM and ATLAS Distributed Computing Operations Shifts (ADCoS) During Summer 2012, UTD joined upgrade activities in preparation for LS1. We took a major role in the testing of Electro-Readout (ER) Bundle testing for new Service Quarter Panels (nSQP?s), and we developed two utilities to measure the timing jitter and bit error rate of the Pixel readout chain for use commissioning Pixel detector upgrades. During BABAR?s heyday, the UTD group pioneered the use of e^+ e^- annihilation events with hard Initial State Radiation (ISR) to study the charm threshold region, and we carried out the first BABAR double-$c\bar{c}$ analysis. Our most recent ISR paper, written in collaboration with A. Palano (Bari) is Exclusive Production of Ds^+ Ds^-, D_S^(*+) Ds^-, and Ds^(*+) Ds^(*-) via e+ e- Annihilation with Initial-State-Radiation was published in Physical Review D 82, 052004 (2010). Work continues on a study of ISR Λc^+ Λc^- production, and a new search to establish and study double-$s\bar{s}$ production is starting.

***K. INTELLECTUAL PROPERTY /**

## Search for Dark Matter using Lepton Jets

The search for dark matter is motivated by the observations from astrophysical experiments, *e.g* HEAT, PAMELA, DAMA/LIBRA, and ATIC. Theorists proposed dark sector models satisfying these observations that can be tested at collider experiments such as the LHC. According to these models the dark matter is charged under a non-abelian dark gauge symmetry that is broken at ~ 1 GeV. The dark matter excited and ground states can transition via the emission of a dark gauge boson (or simply a dark photon) that couples via kinetic mixing to the Standard Model photon, and hence, lepton or quark pairs. These dark photons carry mass in the range from O(100) MeV to O(1) GeV, so they decay primarily into highly-boosted, collimated leptons. The absence of an antiproton excess in astrophysical data limits the dark photon mass to below 2 GeV. The collimated set of energetic leptons forms a lepton-jet that is experimentally accessible. Lepton-jets are also predicted by other new-physics models, *e.g*. a model where the Higgs decays to the dark sector.

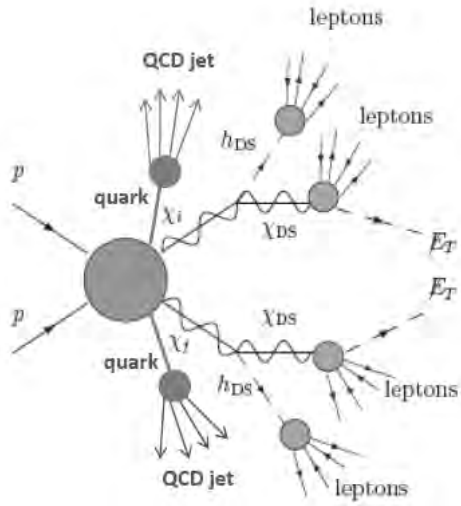


*Fig. 1.* Supersymmetric production of the lepton-jet final state. The lightest neutralino produced in the visible sector is not the lightest supersymmetric particle, but it is allowed to decay into a dark Higgs and dark photons.

During 2011, ATLAS collected about 4.8 $fb^{-1}$ of good quality proton-proton collision data. Ahsan utilized this data to search for evidence of two (or more) prompt lepton jets in the electron channel. The dark photon branching fraction presented in Fig. 3 is determined by the coupling of the SM virtual photon which is determined by low-energy $e^+e^-$ annihilation data. The electron channel is the only kinematically-allowed decay for dark photon masses below the mu-pair threshold. Beyond the mu-pair threshold, electron-jet and muon-jet channels have similar branching fractions, but the mu-pair channel is more sensitive thanks to lower backgrounds.

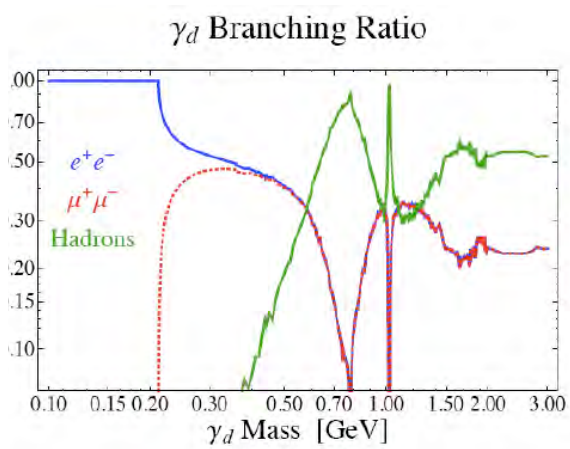


*Fig. 2.* Dark photon branching fraction as a function of dark photon mass

Although the search for two lepton jets final state is sensitive to many exotic models, we concentrate on the final states produced through a Supersymmetry (SUSY) mechanism. These SUSY models are sensitive to $\epsilon$, the coupling of dark photons with Standard Model photons. Values of $\epsilon$ in the range $10^{-3}$ to $10^{-4}$ are consistent with PAMELA and DAMA results . The decay length of a dark photon is

$(2.7\times10^{-6}\ \mu m)/((m_a/GeV/c^2)\epsilon^2)$, which implies that for a dark photon mass $m_a \sim 1\ GeV/c^2$, decays would effectively be prompt for $\epsilon$ values $>10^{-4}$.

Ahsan has developed algorithms for electron-jet reconstruction, and she has defined an analysis strategy for efficient event selections with good discrimination against the background events. Signal efficiency is determined from signal Monte Carlo and checked using samples of leptonic $J/\psi$ decays and converted photons. QCD jets, by virtue of their high production cross section, are the dominant background despite their small probability ($O(10^{-3})$) to fake a pair of collimated electrons. Other background sources are from the production of a photon recoiling against a jet, top quark pair production, and electroweak production mechanisms such as the associated production of a W boson or a Z boson with a jet, or di-boson production. A data-driven technique is used to estimate backgrounds.

Figure 4 shows the expected reconstructed mass distributions for the leading jet $e^+e^-$ pair and the next-to-leading jet $e^+e^-$ pair, for one signal hypothesis, a 150 $MeV/c^2$ dark photon and $\alpha_d$=0.1. The expected signal yield for various values of dark gauge coupling strength, $\alpha_d$ and various dark photon masses are shown in Table 1, together with the expected background level. No electron-jet excess is found in 2011 data, leading to a 95% confidence level upper limit for the production cross section times branching fraction for two prompt electron jets for dark photon masses up to 500 $MeV/c^2$. The electron analysis is most sensitive for dark photon masses below 210 $MeV/c^2$. A draft conference note for this analysis is still

| Dark Sector Hypothesis | Event yield for 4.8 $fb^{-1}$ for $\sqrt{s}$ = 7 *TeV* | Event yield for 15 $fb^{-1}$ for $\sqrt{s}$ = 8 *TeV* |
|---|---|---|
| $\alpha_d = 0.0,\ m_a = 150\ MeV/c^2$ | 110.2 ± 10.9 | 471 |
| $\alpha_d = 0.0,\ m_a = 300\ MeV/c^2$ | 36.8 ± 6.3 | 157 |
| $\alpha_d = 0.0,\ m_a = 500\ MeV/c^2$ | 16.1 ± 4.2 | 69 |
| $\alpha_d = 0.1,\ m_a = 150\ MeV/c^2$ | 143.0 ± 12.4 | 612 |
| $\alpha_d = 0.1,\ m_a = 300\ MeV/c^2$ | 36.1 ± 6.2 | 154 |
| $\alpha_d = 0.1,\ m_a = 500\ MeV/c^2$ | 27.2 ± 5.4 | 116 |
| $\alpha_d = 0.3,\ m_a = 150\ MeV/c^2$ | 138.0 ± 12.2 | 590 |
| $\alpha_d = 0.3,\ m_a = 300\ MeV/c^2$ | 39.9 ± 6.5 | 171 |
| $\alpha_d = 0.3,\ m_a = 500\ MeV/c^2$ | 14.4 ± 3.9 | 62 |
| Expected Background | 15.2 ± 2.7 | ? |

*Table 1: Expected electron jet signal yield and background for the 2011 data (center) and a scaled yield projection of the 2011 values to correspond to the 2012 8 TeV data set (right). The* expected background for the 2012 data requires investigation. The signal-to-background cross section ratio should be larger, but pile-up is larger too, so simple scaling rules don't apply

under review and is not yet public. It is to be combined with results of a parallel search for prompt muon jets in a paper that is targeted for publication this fall.

By the end of 2012, ATLAS is expected to collect in excess of 15 $fb^{-1}$of 8 *TeV* data. The cross-section for squark pair production increases by a factor of 1.37 with the center of mass energy increase from 7 *TeV* to 8 *TeV* as described in reference. The increase in integrated luminosity together with the rise in center of

mass energy will improve the sensitivity for a dark photon search with projected electron-jet events yields shown in the rightmost column of Table 1. The sensitivity for higher-mass dark photons can be increased further by looking for two lepton jets events with both muon-only jets and combinations of muon and electron jets with mass sensitivity up to 2 *GeV*. Additionally, the lepton-jet search can be extended to lower values of the dark-SM coupling $\epsilon$ by searching for lepton jets displaced from the primary vertex.

The reconstruction efficiency of electron jets is an important systematic uncertainty. as the showers associated with the $e^+e^-$ can merge. Photon conversions and $J/\psi$ decays to electrons provide cross checks, however the lepton pair mass is either too high or low, respectively. Namasivayam is studying whether $\phi \rightarrow e^+e^-$ decays from $D_s$ decays can provide a clean alternative. Prompt $\phi$ candidates are known to suffer from QCD backgrounds.

For the 2012 dark photon search. Ahsan replaced E. Strauss (SLAC) as t coordinator, and lead analyst for the muon-jet channel. Namasivayam is lead analyst for the electron-jet channel.

## Search for Charmonium-like *X*, *Y*, *Z* States

In the past decade, over a dozen new charmonium-like (containing $c\bar{c}$) resonances have been observed by *BABAR*, Belle, CLEOc and the experiments at the Tevatron (Table 2). The LHC experiments are now

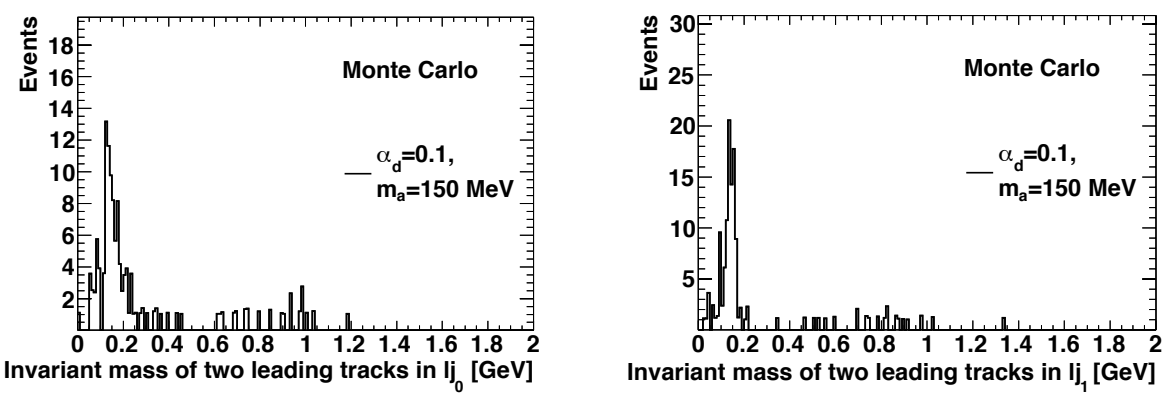


*Fig. 3.* The invariant mass distribution of the two electron tracks in the leading lepton jets (left) and the sub-leading lepton jet (right ) for a dark photon mass of 150 MeV and $\alpha_d$=0.1, normalized for 4.8 $fb^{-1}$ of data.

contributing to this field of study, exploiting the huge data sets provided by the impressive performance of the LHC.

A better understanding of the nature of these new states is needed to constrain or exclude QCD models, and ATLAS, CMS, and LHCb are actively contributing to these studies. ATLAS and CMS share similar properties in terms of their ability to provide differential measurements with respect to pseudorapidity and transverse momentum, with $|\eta| < 2.5$ and $p_T$ values beginning around 8 GeV. LHCb has a different and complimentary reach, with access to pseudorapidity values between 2.5 and 4.5, and $p_T$ values between 5 and 20.

| State | $M$, MeV | $\Gamma$, MeV | $J^{PC}$ | Process |
|---|---|---|---|---|
| $X(3872)$ | $3871.52 \pm 0.20$ | $1.3 \pm 0.6$ | $1^{++}/2^{-+}$ | $B \to K(\pi^+\pi^- J/\psi)$ |
| | | $(< 2.2)$ | | $p\bar{p} \to (\pi^+\pi^- J/\psi) + \ldots$ |
| | | | | $B \to K(\omega J/\psi)$ |
| | | | | $B \to K(D^{*0}D^0)$ |
| | | | | $B \to K(\gamma J/\psi)$ |
| | | | | $B \to K(\gamma\psi(2S))$ |
| $X(3915)$ | $3915.6 \pm 3.1$ | $28 \pm 10$ | $0/2^{?+}$ | $B \to K(\omega J/\psi)$ |
| | | | | $\gamma\gamma \to (\omega J/\psi)$ |
| $X(3940)$ | $3942^{+9}_{-8}$ | $37^{+27}_{-17}$ | $?^{?+}$ | $e^+e^- \to J/\psi(D\bar{D}^*)$ |
| | | | | $e^+e^- \to J/\psi\ (\ldots)$ |
| $Y(4008)$ | $4008^{+121}_{-49}$ | $226 \pm 97$ | $1^{--}$ | $e^+e^- \to \gamma(\pi^+\pi^- J/\psi)$ |
| $Z_1(4050)^+$ | $4051^{+24}_{-43}$ | $82^{+51}_{-55}$ | ? | $B \to K(\pi^+\chi_{c1}(1P))$ |
| $Y(4140)$ | $4143.4 \pm 3.0$ | $15^{+11}_{-7}$ | $?^{?+}$ | $B \to K(\phi J/\psi)$ |
| $X(4160)$ | $4156^{+29}_{-25}$ | $139^{+113}_{-65}$ | $?^{?+}$ | $e^+e^- \to J/\psi(D\bar{D}^*)$ |
| $Z_2(4250)^+$ | $4248^{+185}_{-45}$ | $177^{+321}_{-72}$ | ? | $B \to K(\pi^+\chi_{c1}(1P))$ |
| $Y(4260)$ | $4263 \pm 5$ | $108 \pm 14$ | $1^{--}$ | $e^+e^- \to \gamma(\pi^+\pi^- J/\psi)$ |
| | | | | $e^+e^- \to (\pi^+\pi^- J/\psi)$ |
| | | | | $e^+e^- \to (\pi^0\pi^0 J/\psi)$ |
| $Y(4360)$ | $4353 \pm 11$ | $96 \pm 42$ | $1^{--}$ | $e^+e^- \to \gamma(\pi^+\pi^-\psi')$ |
| $Z(4430)^+$ | $4443^{+24}_{-18}$ | $107^{+113}_{-71}$ | ? | $B \to K(\pi^+\psi(2S))$ |
| $X(4630)$ | $4634^{+9}_{-11}$ | $92^{+41}_{-32}$ | $1^{--}$ | $e^+e^- \to \gamma(\Lambda_c^+\Lambda_c^-)$ |
| $Y(4660)$ | $4664 \pm 12$ | $48 \pm 15$ | $1^{--}$ | $e^+e^- \to \gamma(\pi^+\pi^-\psi(2S))$ |

*Table 2. List of new particles observed in past decade, their properties, and the decay channels in which they have been observed .*

The UTD and Novosibirsk groups on *BABAR* pioneered the Initial State Radiation technique for detecting and studying new hadrons at *b*-factories. We discovered the *Y(4260)* resonance, we were first to report the *Y(4350)* structure, and we confirmed Belle's observation of double $c\bar{c}$ production in $e^+e^-$ annihilations. As members of the Onia Working Group, we are exploring *X*, *Y* physics topics with ATLAS data. Our current focus is on a measurement of the production rate and $p_T$ spectrum of the *ψ(2S)* and the $X_c(3872)$ and expect to complete an ATLAS internal note for Onia Working Group review by the end of 2012. We will then turn to measurement of the properties of other *XYZ* states, with a particular

interest in confirming or refuting the $Z(4430)^-$ observation reported by Belle but was not confirmed by Babar. The $Z(4430)^-$, if confirmed, would be the first known charged state with $c\bar{c}$ content.

**$X(3872) \to J/\psi\pi^+\pi^-$ <u>Analysis</u>**

Wong, Lou, Reeves, and Izen have been working on the $(X, Y) \to J/\psi\pi^+\pi^-$ analysis with ATLAS data. The selection criteria for *X(3872)* have been determined with guidance from Monte Carlo signal samples and the data *ψ(2S)* signal.

Following Wong's Ph.D. thesis in June of 2012, Reeves has assumed the responsibility for completing this analysis and preparing it for publication. He processes AOD data over the grid with the ATLAS Athena analysis code that includes our $J/\psi\pi^+\pi^-$ selection and applies kinematic and vertex fits, producing

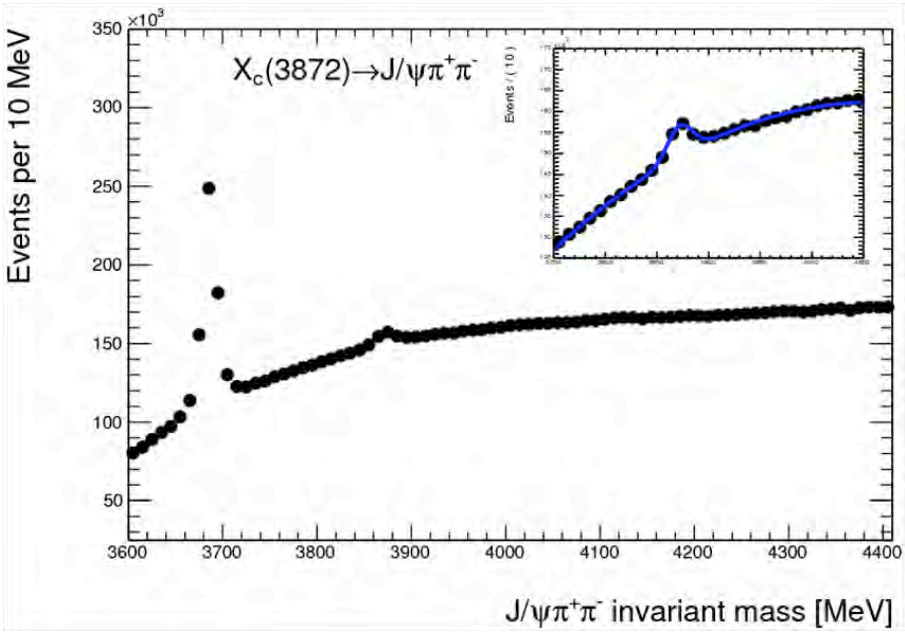


Fig. 5. Evidence for *ψ(2S)* and *X(3872)* production.

nTuples containing the kinematical and detector variables for $\mu^-\mu^-\pi^-\pi^-$ combinations, trigger bits, and generator truth bank information for Monte Carlo simulated events. Lou and Reeves confer several times per week via Internet conferencing to discuss developments and planning.

Candidate $X(3872) \to J/\psi\pi^+\pi^-$ events are selected from ATLAS data collected during 2010 and 2011 for periods up to K4. The resulting $J/\psi\pi^+\pi^-$ mass spectrum, shown in figure 5, shows clear evidence for $\psi$(2S) and $X$(3872) production. Analysis updates have been presented regularly to the ATLAS Onia working group throughout 2011 and 2012. A publication is being targeted for Fall 2012 and will include a measurement of the *X(3872)* production rate and its differential cross section with respect to $p_T$. We are improving the signal fits, measuring detection efficiencies, evaluating systematic errors, fine tuning our discrimination of prompt versus non-prompt production, and making steady progress towards a paper.

## Pixel Run Coordination

Reeves served as the Pixel Deputy Run Coordinator for six months beginning in March 2011, and then in September he took over as Pixel Run Coordinator, and he continued in this position until the end of February 2012. In this capacity he has managed the daily operations of the Pixel detector during the 2011 run; he has represented the Pixel community in the daily ATLAS operations meetings; and he has ensured that needs and concerns of the Pixel community were forwarded within the Inner Detector community as the transition to a single ID shifter was executed.

The LHC had a banner year in 2011, as did ATLAS and the ATLAS Pixel Detector. The LHC delivered

| **Inner Tracking Det.** | | | **Calorimeters** | | | | **Muon Detectors** | | | | **Magnets** | |
|---|---|---|---|---|---|---|---|---|---|---|---|---|
| Pixel | SCT | TRT | LAr EM | LAr HAD | LAr FWD | Tile | MDT | RPC | CSC | TGC | Solenoid | Toroid |
| 99.8 | 99.6 | 99.2 | 97.5 | 99.2 | 99.5 | 99.2 | 99.4 | 98.8 | 99.4 | 99.1 | 99.8 | 99.3 |

*Table 3. Luminosity weighted relative detector uptime and good quality data delivery during 2011 stable beams in pp collisions at √s=7 TeV between March 13th and October 30th (in %), after the summer 2011 reprocessing* campaign

first stable beams on March 13th, colliding 3 bunches in the ATLAS interaction point. By the middle of July the LHC had progressed to filling the accelerator with 1380 bunches spaced by 50 ns, and then regularly provided fills with 1337 bunches colliding for ATLAS. By the end of October, 2011 at the conclusion of the year's proton physics, the LHC had delivered 5.6 $fb^{-1}$. ATLAS was prepared for the stellar performance of the LHC, recording 93.5% of the delivered luminosity.

While all of the subdetectors comprising the ATLAS detector performed well in 2011, the Pixel detector performed especially well, despite the harsh environment in which it operates. As seen in Table 3, the Pixel detector was up and providing good data for 99.8% of the time that stable beams were available during the proton physics program, an achievement unsurpassed by any other detector element, and matched only by the Solenoid magnet.

Finally, November and the first week of December 2011 were devoted to heavy ion physics, with the LHC colliding Pb nuclei and delivering 166 $\mu b^{-1}$, of which ATLAS recorded 158 $\mu b^{-1}$, for an efficiency of 95.1%. This represents a factor of 17 increase over what was recorded during the 2010 heavy ion running. Reeves handed off a working detector to his successor in March, 2012, and 2012 running has been equally successful.

## Pixel Detector and Data Quality Monitoring

Ahsan is responsible for the online monitoring application used by shifters during data taking to visualize the histograms to check data quality. Continual improvements of the online data quality monitoring display application (DQMD), reference plots, and automated monitoring algorithms are required as luminosity keeps increasing. During the Summer 2011, the three inner-detector subsystems, Pixel, Semiconductor Tracker and Transition Radiation Tracker shifts merged their control room shifts. Consequently, the monitoring applications were merged for more convenient use by the single inner detector shifter. The transition went smoothly and involved a complete reorganization of histograms, data quality algorithms and configuration files. Ahsan has provided the wiki-based documentation for DQMD. As an on-call DQM expert shifter, she responds to questions and feedback from both the online and offline shifters. The on-call shifter is responsible for uploading offline mask to the database to treat modules exhibiting noisy front-end electronics, s/he crosschecks the data quality evaluation done by DQM shifters, and s/he signs-off on the data quality flags during the weekly data preparation meeting.

## Future Lifetime of Optoboard StudieS (FLOSS)

In July, 2010, Izen was asked by the Pixel Project Leader, Beniamino di Girolamo to lead an urgent lifetime study of the Pixel Optoboard. The Pixel detector relies on a fiber optic link to transmit commands, configurations, and clock signals from the counting room to the detector on the beam line and to transmit data from the detector back to the counting room. The same custom-for-ATLAS TrueLight Vertical-Cavity Surface-Emitting Lasers (VCSELs) are used on Pixel (and SCT) "TX

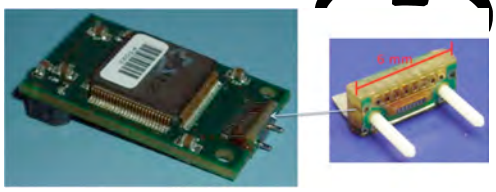

*Figure 6. TX plug-in with TrueLight VCSEL.*

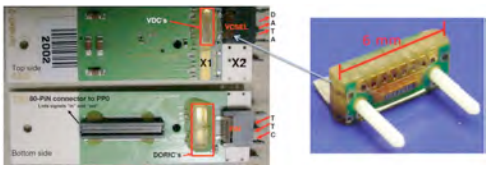


*Figure 7. Optoboard with TrueLight VCSEL.*

plugins" to transmit to the detector with a 50% "half clock" duty cycle, and on the Optoboards to transmit from the pit as needed when Pixel modules have data to report.

The TX-plugin VCSELs in the counting room were failing at an alarming rate. As of December 5, 2010, 223 of 272 VCSELs had failed, and that number grew to 321 failures by November, 2011. During 2011, a pre-emptive program to replace TX-plug-ins for the important inner-most Pixel layer started as the availability of TrueLight plug-ins improved; however, there was great concern that Optoboard VCSELS might fail as well. VCSEL aging and failures were thought to be related to the 'bright time" of VCSELs, but the cause of failures was not known. Narrowing of the optical spectra of VCSELs is a well-known symptom. The ATLAS custom modification of the Distributed Bragg Reflector layer was a suspect. Aging tests had not been performed on production ATLAS-modified TrueLight VCSELs before construction. Problems with early production runs were attributed to poor electrostatic discharge (ESD) precautions by TrueLight and handling by ATLAS. Those problems were corrected, but VCSEL failures emerged during operations. The projection for on-detector failures shown in Fig. 8 was based on the death rate of TX-plugin VCSELs in the counting room. The projection takes into account the increasing duty cycle of Optoboard VCSELs as the LHC luminosity increases. It suggested that we might expect to see the onset of on-detector VCSEL failures as early as 2015.

ATLAS has been preparing for a possible Pixel intervention during LS1 in 2013 pending guidance from aging tests, including Izen's FLOSS study, that were started in 2010 and 2011. In an intervention, the Pixel service quarter panels and their optoboards would be replaced by a new design (nSQP), which would transport signals to/from the detector electrically via twisted pairs to redesigned Optoboards. The replacement Optoboards would be located outside of the inner detector volume in a serviceable location.

Several aging studies were instituted within the Pixel group. The FLOSS study was led by Izen with help from Stanford student Katie Malone. The operational start for FLOSS was August 2010. FLOSS was comprised of 53 VCSEL channels on 8 Optoboards. The study used 7 of the 14 ½-staves of modules of the Pixel group's ToothPIX prototype (note the oral hygiene theme) which is maintained in the SR-1 building at CERN for DAQ development and training purposes. The FLOSS study was being carried out with the same 50% ½-clock cycle that the TX-plugins transmit. The urgency of a developing problem dictated a quick start in 2010 with existing equipment; however the goal was to separate FLOSS from ToothPIX' DAQ, slow control and service infrastructure. Contention between ToothPIX and FLOSS was a persistent operational problem. Izen assembled the hardware components required to run FLOSS as a standalone detector. The Siamese twins were separated in April 2011.

With FLOSS separated from the complex ToothPIX infrastructure, Izen wrote and implemented an automated CRON job that ran on the Single Board Computer (SBC) in the FLOSS VME crate. Every 10 minutes, voltages sensitive to whether aging was ongoing were recorded, and the level of light received from the FLOSS optoboards by the "RX" pin diode was measured. Malone wrote the interface to produce summary charts such as the sample shown in Fig. 9, plus scripts to calculate the aging time for each FLOSS VCSEL. LOSS aging was interrupted periodically to record optical spectra, and this direct measurement was the most reliable means to establish a TX death. As VCSELs age, they typically develop a narrowed spectrum, although the narrowing is hard to quantify for multi-mode lasers, which have irregular spectra. Izen detected the FLOSS "Optodeath" shown in Fig. 10, during optical scans on

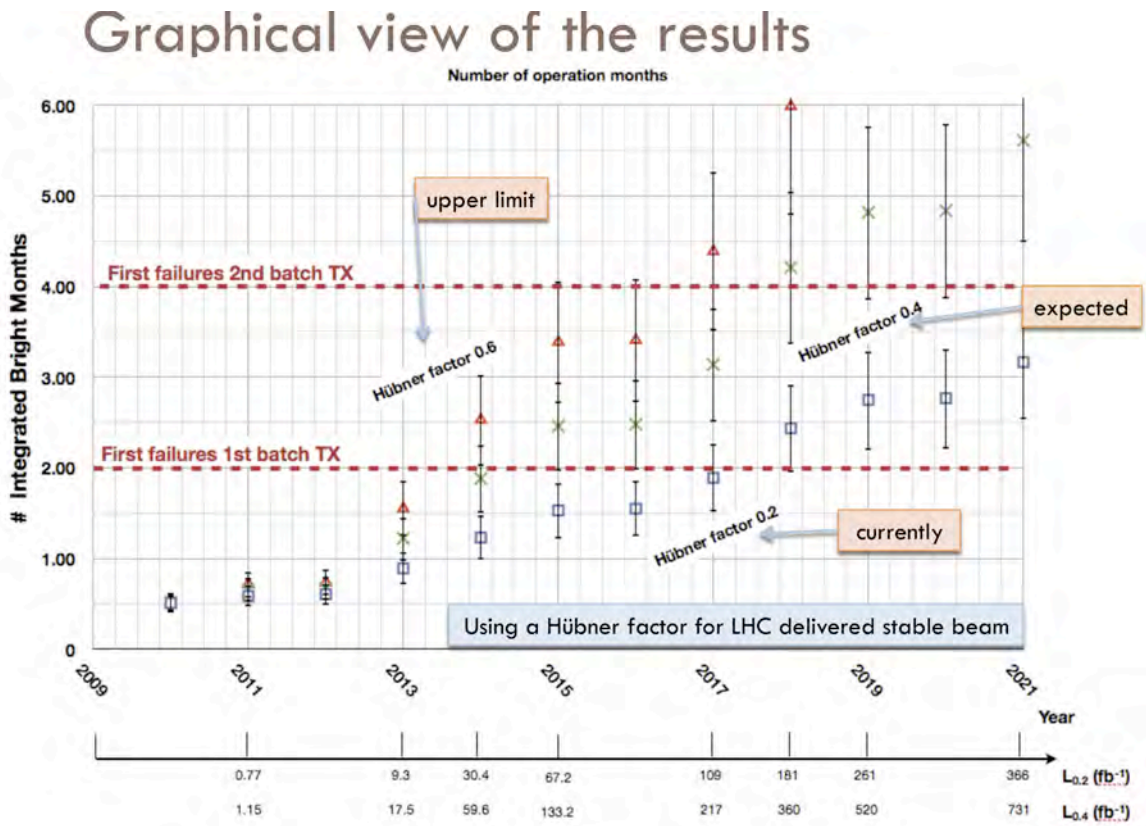


*Figure 8. Estimated bright time of on-detector VCSELs with time and integrated luminosity. The onset of TX-plugin failures are shown by the dashed red lines. (Estimate by Beniamino di Girolamo)*

January 18, 2011 after ~4 months of FLOSS bright time. This was the sole optodeath during the study. The 300-day bright time of FLOSS VCSELs more than doubled the projection for the lifetime of on-detector VCSELS.

Results from FLOSS (and other studies) suggest that the optoboard VCSELs will outlast the detector. Other studies suggested that humidity was the culprit contributing to the TX VCSEL deaths in the counting room. Counting room TX plugins have now been replaced using VCSELs from another manufacturer.

## On-Detector Aging Studies

While working with FLOSS, Izen noticed a peculiar behavior of the Optoboards. When the DC supply voltages supplied to a Pixel module's front end electronics are unpowered or "disabled", the corresponding VCSEL state is unspecified. It turns out that pick-up from the clock signal triggers the VCSEL driver! This was not intended, nor even realized by the Pixel community. The identical behavior, first observed by Izen in FLOSS, has been confirmed for on-detector VCSELs in the pit. Approximately 35 of the 1744 on-detector Pixel modules have been disabled, but have healthy VCSEL channels. These channels are thought to have been aging since the detector was first turned on, and may prove to be the most realistic VCSEL aging study of all. A regular program to monitor the optical spectra of all 1744 on-detector VCSEL modules was instituted. Several days of optical spectrum shifts are required to characterize the whole detector. Izen was part of the team that first completed these measurements in February, 2011, and again when measurements were repeated in July 2011. They were re-measured in January 2012. Study of the "disabled" channels that continually transmit by M. Cooke (LBNL) found

stable optical spectra with few signs of aging. This is consistent with other studies that demonstrate that the TrueLight VCSEL vulnerability is humidity.

The ATLAS Inner Detector volume is bathed in dry Nitrogen, so humidity is not a factor for our on-detector components. Pixel detector VCSELS are expected to outlast the rest of the Pixel detector. A decision on whether to extract the Pixel detector for servicing during the 2013 long shutdown will likely be taken in October, 2012. Repair of defective channels, and simplified installation of the Insertable B (Pixel) Layer (IBL) are the considerations that might warrant the risk of removing the Pixel detector from ATLAS, although installation of the nSQPs appears likely if the detector is extracted. Beyond 2013, the PIXEL detector will no longer be serviceable as it will become to radioactive to handle safely.

## Long Shutdown 1 and Scientific Associate Plans

During the 2013–2014 shutdown, Izen anticipates playing an active role in the commissioning of the IBL and, if installed, the new Service Quarter Panels. He plans to be at CERN during the Summers of 2013 and 2014, both of which occur during LS1. He is preparing an application for a CERN Scientific Associateship with the encouragement of the Pixel Project Leader and Technical Coordinator-designate, B. di Girolamo and others in the Inner Detector community. His proposed project would be to coordinate the integration of the Pixel nSQP in the likely event that ATLAS elects to replace the existing Service Quarter Panels. Otherwise, he would integrate the IBL into existing calibration and diagnostic scan software for the Pixel detector. Time permitting, the "Calibration Console" GUI may be redesigned to make the interface easier for non-experts.

## Pixel DAQ Software Coordination

Reeves assumed responsibility as the On-site Pixel DAQ Software Coordinator in 2010 and served through June 2012. He instituted weekly meetings for the Pixel code developers and experts. Under Reeves' leadership, the improved organization and communications attracted new participants, doubling the size of the Pixel DAQ community within half a year. In October 2011, the Pixel and the Pixel Insertable B-Layer online software communities were merged to avoid duplication of effort. The combined group has achieved a size sufficient to ensure that most projects that have been identified are assigned to at least one developer.

Accomplishments during 2011 include:

- The deployment of a process allowing for individual pixel modules to be reconfigured and then included back into data taking without the need to interrupt ATLAS data-taking. Previously, modules lost to Single Event Upsets (SEU) would only be available for taking data with the next ATLAS run.
- A refactoring of software classes to cleanly separate histogramming operations from the hardware controlling these operations. This promises to make the Pixel detector both more robust and more efficient during data taking by moving monitoring and recovery interventions from external processes running on DAQ PCs to the Read Out Drivers (RODs) through which the Pixel data is flowing.

- Integration of the Doxygen and Coverity tools into the Pixel DAQ code, the authorship qualification project of UTD student Namasivayam.

Reeves' personal contributions have been primarily in providing DAQ software documentation and the development a new tool for ensuring that the Pixel modules are in a safe state for LHC injection.

The DAQ software coordinator is ultimately responsible for delivering DAQ software releases. Reeves worked with Paolo Morettini (INFN Genoa), the Pixel group's lead developer and DAQ guru, to build and test releases on the ToothPIX prototype before validating them with the full detector. In a perfect world, this would be an orderly process. On occasion, emergency fixes were required to address beam backgrounds and pathological problems. Eighty million channels in close proximity to the beam pipe present some of the most challenging DAQ problems in all of ATLAS. In addition to overseeing the DAQ group, Reeves' personal contributions have been primarily in providing DAQ software documentation and the development a new tool for ensuring that the Pixel modules are in a safe state for LHC injection. As a DAQ on-call expert shifter, he is called upon to troubleshoot nasty problems in real time that have been known to cause the entire ATLAS DAQ system to go busy.

## Pixel Service Quarter Panel Upgrade

Amid concern about the longevity of the on-detector Service Quarter Panel (SQP) optoboards in 2010, ATLAS initiated the new Service Quarter Panel (nSQP) project. The nSQP's replicate the functionality of the current SQPs which route power, cooling, and data for the ATLAS Pixel Detector, but they introduce an additional step in the electro-readout. Current SQPs use their optoboard VCSELs to transmit data directly from the detector to the Counting Room via optical fibers. In the nSQP design, twisted-pair wires, collected into Electro-Readout (ER) bundles, carry electrical signals out of the Inner Detector volume. Redesigned optoboards at this more-easily-serviced location restore the readout chain and transmit optical signal to the Counting

Room. While the most serious concerns regarding VCSEL lifetime has been allayed, the nSQP project provides the option to repair channels which have failed for other reasons.

University of Texas at Dallas students Brandyn Lee and Jessica Smith were part of the nSQP production team during their first visit to CERN this past summer. They performed qualification tests on ER bundles, inspecting the cable and the connector boards attached to each end of the bundles for shorts, and the connectors were visually inspected for cold-solder joints. As each ER bundle contains multiple twisted pairs, they tested to make sure each wire was properly soldered to the correct places on the cable and connector boards. They tested the electrical connection of the cable shielding to the connector boards, and they made capacitance measurement. Finally, they tested the quality of signals transmitted through each twisted pair.

Additionally, Lee and Smith wrote utility programs providing new tests for use in ensuring the quality and setup of the modified electro-readout system. Lee's BitErrorRate program sends streams of data to the module controller chip on the nSQP through the electro-readout chain and then reads the data back for an error rate determination. Smith's program measures the jitter introduced by the readout.

They've documented their programs on the Pixel ReadOut Driver Utility (RodUtil) Twiki.

**Final Scientific/Technical Report for the Theory Part of Grant Number:** DE-FG02-04ER41310

**Title of the Theory Part:** Tests to Investigate Dark Energy versus Modified Gravity Models

**Type of project:** Theory – Dark Energy

**DOE/Office of Science Program**

**Office:** High Energy Physics

**DOE Contact**: Dr. David Boehnlein 301-903-7843

David.Boehnlein@science.doe.gov

**Principal Investigator for the Theory Part:**

Dr. Mustapha Ishak-Boushaki
Department of Physics
University of Texas at Dallas
800 Campbell West Road
Richardson, TX, 750830688
Telephone number: 972-883-2815
Email: mishak@utdallas.edu

**Institution:**

The University of Texas at Dallas
800 Campbell West Road
Richardson, TX, 750830688

**Final Scientific/Technical Report for the Theory Part of the Project:** DE-FG02-04ER41310
Dark Energy Theory: Tests to Investigate Dark Energy versus Modified Gravity Models

**Executive summary:** In this project, we investigated tests that can be used in order to determine whether cosmic acceleration is due to the effect of Dark Energy in the universe, or, the result of the modification to gravity physics at large scale of distances. We developed tests using the dynamical equations and implemented them into numerical codes. We then applied them to the most recent cosmological data sets. We used in our approach the fact that Dark Energy affects the expansion rate of the universe and also the growth rate of large-scale structure in the universe (the growth of cosmological structures like clusters of galaxies). We developed and used parameterizations that will signal any departure from models of Dark Energy. We have shown that, for now, a prevalent Dark Energy component in the universe is the most plausible explanation for cosmic acceleration. However, we also found that modified gravity models cannot be excluded for now, and more precise future data is required to do so. Our results have been communicated in 9 scientific journal publications, 15 conference presentations, and 1 software available on the internet for the scientific community working on the question of Dark Energy. The project allowed the training of two graduate students. One of them finished his Ph.D. and is now a researcher at Queensland University. The codes developed are available to the scientific community working on Dark Energy. The cite has received 970 hits and 80 downloads. The work done and results obtained can be summarized as follows:

- We derived more precise parametrizations for the growth factor index parameter when spatial curvature is accounted for, and compared the new parameterizations to available data (Gong; Ishak; Wang, ***Physical Review D*** 80, 023002 (2009).)
- We proposed a new parameterization of the growth factor index that is free of any physical discontinuities. This was done using analytical functions that smooth the transitions in the redshift space. We showed that not only the index parameter is able to distinguish between Dark Energy and modified gravity, but the slope of the index function constitutes a second distinguishing test (Ishak; Dossett, ***Physical Review D*** 80: 043004 (2009).)
- We used redshift dependent parametrizations of the growth index and compared Dark Energy models and DGP modified gravity models to available cosmological data. We found that the parameterizations used were able to provide significant constraints and rule out background models when incorrectly assumed in the analysis. This analysis also highlighted the caveats resulting from using growth data that has been reduced with the assumption of a given theory or model like the Friedmann models (Dossett; Ishak; Moldenhauer; Gong; Wang, ***Journal of Cosmology and Particle Astrophysics*** 1004: 022 (2010)).
- We conducted a thorough analysis using various data sets in order to probe any deviations from Dark Energy + general relativity models at cosmological scales. The Figure of Merit approach was used to study and compare the constraining power of various combinations of the data sets. The parameterizations and binning methods used showed that the values corresponding to Dark Energy + general relativity are within the 95% confidence level contours for all data set combinations. Some interference between the data sets due to systematic effects was also found during the analysis (Dossett, Moldenhauer, Ishak, ***Physical Review D*** 84, 023012, (2011)).
- We analyzed the *f(G)* modified gravity models as a substitute of Dark Energy. We found that the models can fit the data well and do pass some physical acceptability condition. The

problem with these models though comes from some instability to matter perturbations (Moldenhauer; Ishak; Thompson; Easson, ***Physical Review D*** 81: 063514 (2011)).

- We developed for the investigation a software package called ISiTGR (**I**ntegrated **S**oftware in **T**esting **G**eneral **R**elativity). The software allows the cosmology community to perform tests to distinguish between Dark Energy versus Modified Gravity. The software constitutes an integrated set of modified program modules for the publicly available packages CAMB [Lewis, Challinor, and Lasenby, 2000] and CosmoMC [Lewis and Bridle, 2002]. Two state-of-the-art programs used for cosmological comparisons to the data. ISiTGR also incorporates a modified version to the Integrated Sachs-Wolfe (ISW)-galaxy cross correlations module of [Ho et al., 2008; Hirata et al., 2008] and includes our weak-lensing likelihood module for the recently refined COSMOS weak-lensing tomography data [Schrabback et al., 2010]. Recently we updated the package to include curved models [Dossett and Ishak, 2012]. Using the site tracking tool, statcounter.com, we can see that since its initial public release to the scientific community on September 2011, the ISiTGR website (www.utdallas.edu/~jdossett/isitgr) has been visited 970 times and the software has been downloaded for a total of 80 times at present time. We are aware that at least 4 groups have been using the software for their work on this topic (Dr. Kuntz's group, Oxford, UK; Prof. Tereno's group, Portugal; Prof. Popa's group, Romania; Dr. Melchiorri's group, Spienza, Italy). We continually update the software with newly released data sets and more capabilities. New results and frameworks from this proposed investigation will be added to ISiTGR and made available for use by the scientific community**.** (Dossett; Ishak; Moldenhauer. ***Physical Review D*** 84, 123001 (2011).
- It is well known that allowing for spatial curvature affects constraints on cosmological parameters such as the Dark Energy equation of state parameters. Here we studied the effect of curvature on constraints on parameters used to test Modified Gravity and General Relativity at cosmological scales, commonly known as modified growth (MG) parameters. Using the latest cosmological data sets we find that MG parameters are correlated with the curvature parameter $\Omega_k$ and the constraints on the MG parameters are weakened compared to when $\Omega_k$ is not included in the parameter analysis. We found that the assumption of a spatially flat model on a spatially curved universe does indeed cause an artificial shift in the constraints on the MG parameters, in some cases even producing an apparent deviation from Dark Energy + relativity. (Dossett; Ishak, ***Physical Review D***, 86, 103008 (2012).
- We studied the robustness of the tests to the presence of Dark Energy density and anisotropic stress perturbations. We found that the dispersion in the growth index parameter remains small enough to distinguish between extreme cases of DE models and some commonly used modified gravity models. The sign of the slope of the index parameter remains as solid additional test. Next, we studied the effect of DE perturbations on the modified growth (MG) parameters that enter the perturbed Einstein equations. We find that while the dark energy perturbations slightly affect the MG parameters, the deviations remain small compared to those due to modified gravity models. Additionally, the deviations due to DE perturbations occur at scale ranges that are completely different than those due to some modified gravity models. In summary, we found that the currently proposed cosmological tests to distinguish between DE and modified gravity are robust to DE perturbations even for extreme cases. This is certainly the case even for DE models with equations of state of DE that fall well outside of current cosmological constraints. (Dossett; Ishak; under review at ***Physical Review D*** (2013).

In summary, we feel that our investigation has fulfilled its main objectives, and our work has allowed making progress toward a better delineation of possible causes of cosmic acceleration and Dark Energy.

**Ishak-Boushaki's theory group personnel during the duration of the award:**

Associate professor Mustapha Ishak-Boushaki (theory PI) spent 100% of his research time working on the questions of Dark Energy and cosmic acceleration.

Graduate students:

Jason Dossett, Ph.D. student. Now researcher at Queensland University in Australia.
Worked on tests to distinguish Dark Energy and Modified Gravity.

Jacob Moldenhauer, Ph.D. student. Now assistant professor at University of Dallas.
Worked on f(G) models of Dark Energy/cosmic acceleration.

Austin Peel, Ph.D. student. Graduation planned for May 2015.
Working on Dark Energy and cosmic acceleration questions.

Michael Troxel , Ph.D. student. Graduation planned for May 2014.
Working on Dark Energy and gravitational lensing.

## ACCOMPLISHMENTS:

**1) Parameterizations of the growth of structure as a test to distinguish between Dark Energy and modified gravity models I: New Contiguous Parameterizations and Constraints from current and future data.** Ishak; Dossett. 2009. "Contiguous redshift parameterizations of the growth index". ***Physical Review D*** 80: 043004 (2009).

Abstract: The growth rate of matter perturbations can be used to distinguish between different gravity theories and to distinguish between dark energy and modified gravity at cosmological scales as an explanation to the observed cosmic acceleration. We suggest here parameterizations of the growth index as functions of the redshift (see Caption of figure below). The first one is given by that interpolates between a low/intermediate redshift parameterization and a high redshift, constant value. For example, our interpolated form *γ(z)* can be used when including the CMB to the rest of the data while the late time form can be used otherwise. It is found that the parameterizations proposed achieve a fit that is better than 0.004% for the growth rate in a Lambda-CDM Dark Energy model, better than 0.014% for Quintessence-Cold-Dark-Matter (QCDM) models, and better than 0.04% for the flat Dvali-Gabadadze-Porrati (DGP) model (with Omega_m^0=0.27 for the entire redshift range up z_CMB. We find that the growth index parameters take distinctive values for dark energy models and modified gravity models, e.g. (0.5655,-0.02718) for the Lambda-CDM model and (0.6418,0.06261) for the flat DGP model. This provides a means for future observational data to distinguish between the models.

Figure: Growth index parameter functions for one example of modified gravity model that can act as an alternative t to Dark Energy models. LEFT PART: Shows that it is a very precise parameterization. RIGHT PART: Shows very little dispersion around the γ=11/16=0.687 for DGP models. This will be important to distinguish them from Dark Energy models.

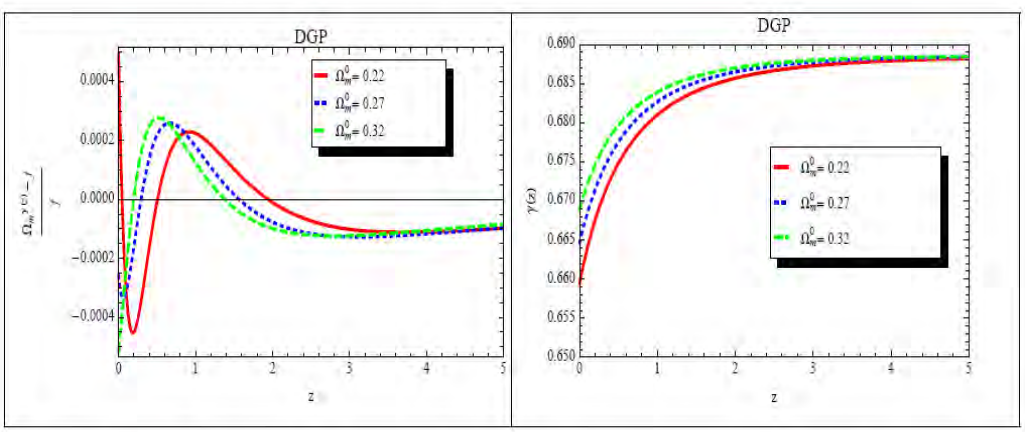


FIG. 2: DGP models. LEFT: We consider the DGP model and plot the relative error $\frac{\Omega_m^{\gamma(z)}-f}{f}$ in order to compare the fit of the proposed parameterization to that of the growth rate $f_{num}$ that is numerically integrated from the growth ODE. We find the best fit parameters $\gamma_0 = 0.6418$ and $\gamma_a = 0.06261$ for $\Omega_m^0 = 0.27$ when $\gamma_\infty^{DGP} = 11/16$. The fit approximates the growth function $f$ to better than 0.04% while the best fit constant $\gamma_{const}^{DGP} = 0.6795$ approximates the growth to 1.95%. So using our redshift dependent parameterization of the growth index provides an improvement to the fit of about a factor 50 for the DGP model. RIGHT: We plot $\gamma(z) = \tilde{\gamma}(z)\ \frac{1}{1+\frac{1+z}{1+z_{ttc}}} + \gamma_\infty^{DGP}\ \frac{1}{1+\frac{1+z_{ttc}}{1+z}}$ for various values of $\Omega_m^0$ showing very little dispersion of the order 0.01 or less at any redshift.

… Continued: Growth index parameter functions for various Dark Energy models
LEFT PART: Shows that it is a very precise parameterization. RIGHT PART: Shows very little dispersion around the γ=6/11=0.545 for Dark Energy models. This confirms that the parameterization is able to distinguish between Dark Energy models and Modified gravity because the values are distinct and the dispersion around the respective values is very small.

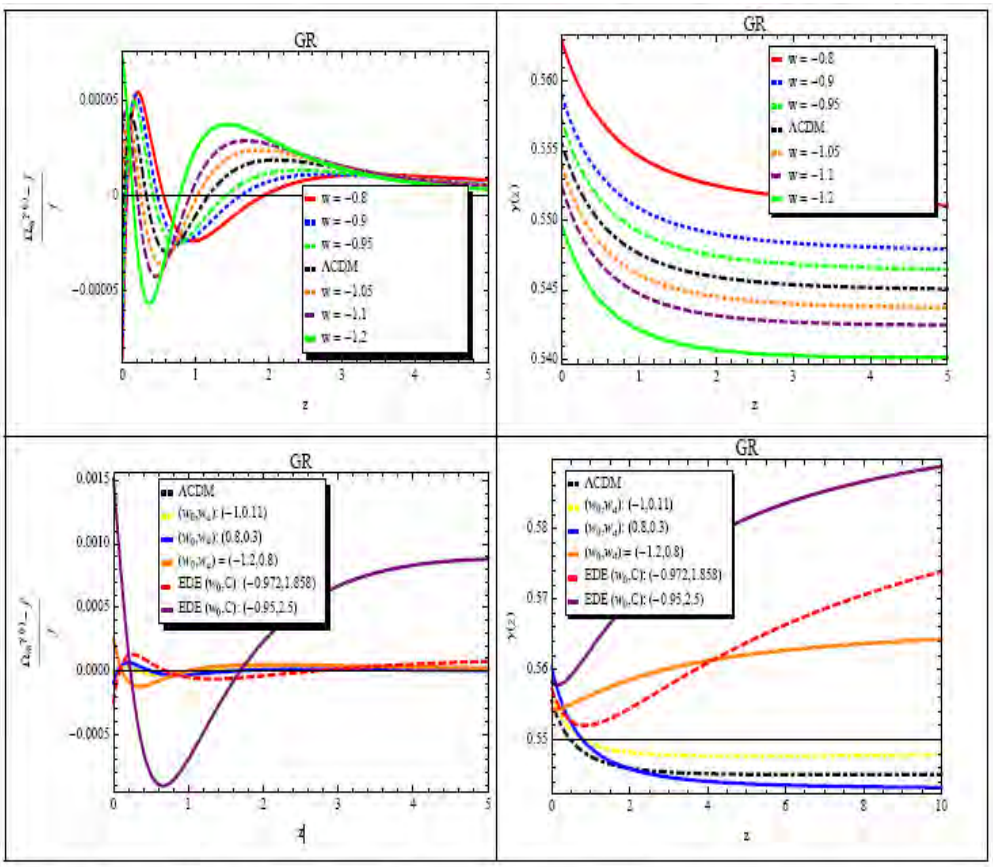


FIG. 1: GR - Dark Energy Models. TOP LEFT: We consider the QCDM models with a constant equation of state and plot the relative error $\frac{\Omega_m^{\gamma(z)}-f}{f}$ in order to compare the fit of the proposed parameterization to that of the growth rate, $f$, that is numerically integrated from the growth ODE. For the ΛCDM, we find the best fit parameters $\gamma_0 = 0.5655$ and $\gamma_a = -0.02710$ when $\gamma_\infty^{\Lambda CDM} = 6/11$. The fit approximate the growth function $f$ to better than 0.004% while the best fit constant $\gamma_{const}^{\Lambda CDM} = 0.5509$ approximates the growth to 0.6%. Using our redshift dependent parameterizations of growth index provides an improvement to the fit of the growth of about a factor 150. TOP RIGHT: We plot $\gamma(z) = \tilde{\gamma}(z)\,\frac{1}{1+\frac{1+z}{1+z_{ttc}}} + \gamma_\infty\,\frac{1}{1+\frac{1+z_{ttc}}{1+z}}$ for various values of the constant equation of state $w$ showing very little dispersion of the order of 0.015 at any given redshift. BOTTOM LEFT:We consider the QCDM models with a variable equation of state, as well as some Early Dark Energy models and plot the relative error $\frac{\Omega_m^{\gamma(z)}-f}{f}$ in order to compare the fit of the proposed parameterization to that of the growth rate, $f$, that is numerically integrated from the growth ODE. We find using our redshift dependent parameterizations of the growth index are able to approximate the growth to within 0.15%. BOTTOM RIGHT: We plot $\gamma(z) = \tilde{\gamma}(z)\,\frac{1}{1+\frac{1+z}{1+z_{ttc}}} + \gamma_\infty\,\frac{1}{1+\frac{1+z_{ttc}}{1+z}}$ for various dark dnergy models with a varying equation of state $w(a)$ including some early dark energy models.

**2) Parameterizations of the growth of structure as a test to distinguish between Dark Energy and modified gravity models II:** Constraints from the latest available data sets and the study of the constraining power of various combinations. Gong; Ishak; Wang. "Growth factor parameterization in curved space". ***Physical Review D*** 80, 023002 (2009). Dossett; Ishak; Moldenhauer; Gong; Wang. "Constraints on growth index parameters from current and future observations". ***Journal of Cosmology and Particle Astrophysics*** 1004: 022 (2010)

**Abstract:** We use current and future simulated data of the growth rate of large scale structure in order to put constraints on the growth index parameters. We use a recently proposed parameterization of the growth index that interpolates between a constant value at high redshifts and a form that accounts for redshift dependencies at small redshifts. We also suggest here another parameterization with an exponential flattening, which tends to the asymptotic value of the growth index for redshifts z>z_ttc, and is found to achieve a fit of the growth factor function for the Lambda-CDM to better than 0.016% for the full redshift range up to the CMB surface. Using these redshift parameterizations or a constant growth index, we find that current available data from galaxy redshift distortions and Lyman-alpha forests is unable to put significant constraints on any of the growth parameters. For example both LCDM and flat DGP are allowed by current growth data. We use an MCMC analysis to study constraints from future growth data, and simulate pessimistic and moderate scenarios for the uncertainties. In both scenarios, the parameterizations discussed are able to provide significant constraints and rule out background models when incorrectly assumed in the analysis. The values taken by the constant part of the parameterizations as well as the redshift slopes are all found to significantly rule out an incorrect background. We also find that an assumed constant growth index over the full redshift range is able to rule out incorrect models but the slopes of redshift dependent parameterizations provide a second test to distinguish between Dark Energy and Modified Gravity.

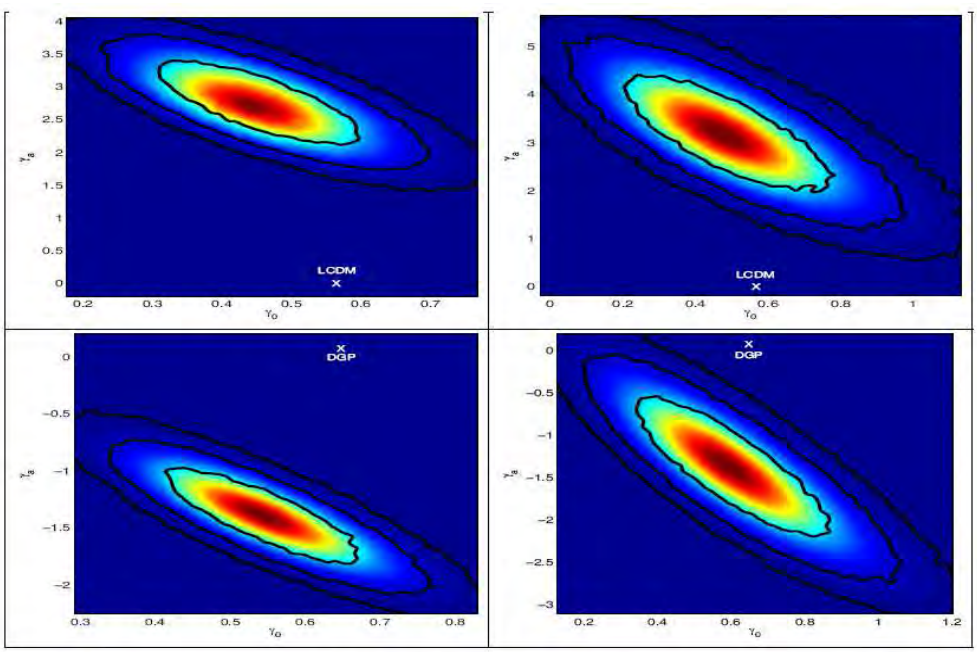


FIG. 3: Interpolated parameterization. TOP LEFT: Moderate scenario fitting fiducial DGP data on an assumed LCDM background. TOP RIGHT: Pessimistic scenario fitting fiducial DGP data on an assumed LCDM background. BOTTOM LEFT: Moderate scenario fitting fiducial LCDM data on an assumed DGP background. BOTTOM RIGHT: Pessimistic scenario fitting fiducial LCDM data on an assumed DGP background. As shown on the figures, in each case the incorrect assumed background model is ruled out to 99.7%.

**3) Exploring the Dynamics and Phenomenology of Higher order invariants models as an alternative to Dark Energy models.** Moldenhauer; Ishak; Thompson; Easson. "Supernova, baryon acoustic oscillations, and CMB surface distance constraints on f (G) higher order gravity models". ***Physical Review D*** 81: 063514 (2011).

Abstract: We consider recently proposed higher order gravity models where the action is built from the Einstein-Hilbert action plus a function $f(G)$ of the Gauss-Bonnet invariant. The models were previously shown to pass physical acceptability conditions as well as solar system tests. In this paper, we compare the models to combined data sets of supernovae, baryon acoustic oscillations, and constraints from the CMB surface of last scattering. We find that the models provide fits to the data that are close to those of the LCDM concordance model. The results provide a pool of higher order gravity models that pass these tests and need to be compared to constraints from large scale structure and full CMB analysis.

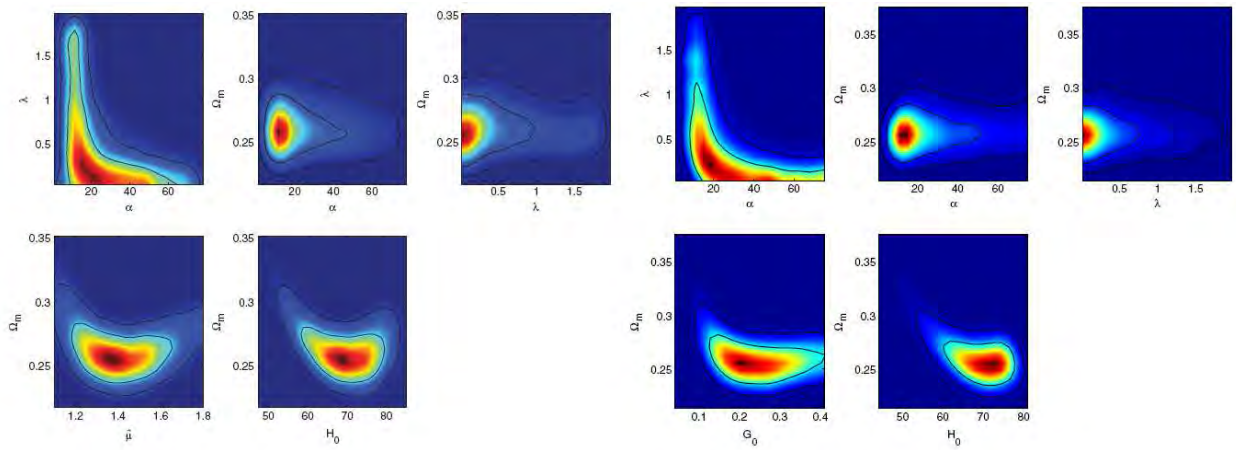

FIG. 1 (color online). Left: $2D$ joint contour plots for DFT-A with parameters $\Omega_m$, $\alpha$, $\lambda$, $\hat{\mu}$, $H_0$ for Union, WMAP5, and SDSS LRG (BAO) data sets, where the inner and outer loops are 68% and 95%, respectively. Right: $2D$ joint contour plots for DFT-A with parameters $\Omega_m$, $\alpha$, $\lambda$, $G_0$, $H_0$ for Union, WMAP5, and SDSS LRG(BAO) data sets, where the inner and outer loops are 68% and 95%, respectively.

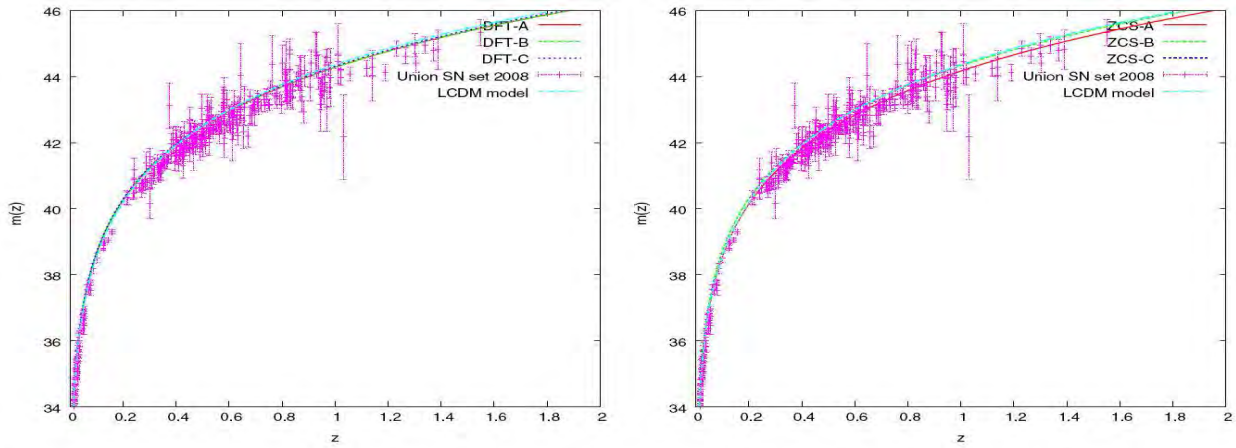


FIG. 4 (color online). Comparisons of different SNe Ia plots with Union data and different values of $f(G)$ models. Left: Comparison of DFT-A, DFT-B, DFT-C Models, and LCDM. Right: Comparison of ZCS-A, ZCS-B, ZCS-C Models, and LCDM.

**4) Figures of merit approach and constraints on Dark Energy versus Modified gravity using latest cosmological data sets:** We studied the constraining power of various combinations of data sets using figure of merit approach (i.e. searching and finding the most sensitive combinations of the data to distinguish between Dark Energy and Modified Gravity)
Journal-ref: Published ***in Physical Review D*** 84, 023012, 2011

**Abstract:** We use cosmological constraints from current data sets and a figure of merit approach (FoM) in order to probe any deviations from Dark Energy + GR models at cosmological scales. The FoM approach is used to study and compare the constraining power of various combinations of data sets on the growth parameters. We use the recently refined HST-COSMOS weak lensing tomography data, the ISW-galaxy cross correlations, the matter-power spectrum from SDSS-DR7, the WPMAP7 temperature and polarization spectra, the BAO from 2DF and SDSS-DR7, and the Union2 compilation of type Ia supernovae, in addition to other bounds from Hubble parameter measurements and Big Bang Nucleosynthesis. We use various parameterizations of the growth parameters that enter the perturbed field equations. We use recently suggested functional forms for the parameters as well as a binning method in order to allow for variations of the parameters with the redshift and scale. We find that the strongest constraints on the growth parameters from current data come from the ISW effect. The parameterizations and binning methods used show that the values corresponding to Dark Energy+ GR are within the 95% confidence level contours for all data set combinations. We find that, in most cases, adding WL data on the top of CMB+MPK makes the constraints weaker, indicating perhaps some interference between the data sets. We do not find any deviation from Dark Energy+GR using the refined HST-COSMOS data.

| Constraints for the parameters $\{Q_{0,\infty}, R_{0,\infty}, D_{0,\infty}\}$ | | | | | | | | |
|---|---|---|---|---|---|---|---|---|
| $k_c = \infty$ | | | | | | | | |
| Dataset | $Q_0$ | $R_0$ | $D_0$ | $Q_\infty$ | $R_\infty$ | $D_\infty$ | $\mathrm{FOM}_{Q_0;R_0}$ | $\mathrm{FOM}_{Q_0;D_0}$ |
| CMB, MPK | [0.69, 2.79] | [−0.34, 2.04] | [0.79, 1.62] | – | – | – | 5.53 | 8.81 |
| CMB, ISW | [0.70, 2.76] | [−0.33, 1.85] | [0.79, 1.55] | – | – | – | 6.15 | 9.80 |
| CMB, WL | [0.57, 2.54] | [−0.30, 2.24] | [0.76, 1.47] | – | – | – | 6.44 | 12.15 |
| CMB, ISW, WL | [0.67, 2.53] | [−0.33, 1.84] | [0.75, 1.34] | – | – | – | 8.46 | 14.96 |
| CMB, MPK, ISW | [0.80, 2.73] | [−0.35, 1.62] | [0.76, 1.46] | – | – | – | 7.53 | 11.97 |
| CMB, MPK, WL | [0.73, 2.80] | [−0.34, 2.13] | [0.82, 1.65] | – | – | – | 5.08 | 7.96 |
| CMB, MPK, ISW, WL | [0.83, 2.82] | [−0.37, 1.60] | [0.77, 1.56] | – | – | – | 7.09 | 10.06 |
| $k_c = 0.01$ | | | | | | | | |
| Dataset | $Q_0$ | $R_0$ | $D_0$ | $Q_\infty$ | $R_\infty$ | $D_\infty$ | $\mathrm{FOM}_{Q_0;R_0}$ | $\mathrm{FOM}_{Q_0;D_0}$ |
| CMB, MPK, ISW, WL | [0.55, 3.24] | [−0.77, 1.71] | [0.31, 1.56] | [0.51, 4.02] | [−0.84, 2.25] | [0.27, 2.01] | 4.06 | 4.72 |

TABLE I: 95% C.L. for the parameters $Q_0$, $R_0$,$D_0$, $Q_\infty$, $R_\infty$, and $D_\infty$ in the first parameterization [70]. For these constraints, we marginalize over the parameter $s$ which characterizes the redshift (time) dependence of the parameterization.

| Inferred parameter constraints on the parameters $\mathcal{G}_{DL}$, $\Sigma_{\mathtt{MGCAMB};1}$ and $\mathcal{V}_{DL}$, $\mu_{\mathtt{MGCAMB};1}$ from parameters $Q_0$, $R_0$, and $D_0$ | | | |
|---|---|---|---|
| Dataset | $\mathcal{G}_{DL}$,$\Sigma_{\mathtt{MGCAMB};1}$ | $\mathcal{V}_{DL}$,$\mu_{\mathtt{MGCAMB};1}$ | $\mathrm{FOM}_{\mathcal{G};\mathcal{V}}$ |
| CMB, MPK | [0.79, 1.62] | [−0.90, 1.79] | 8.81 |
| CMB, ISW | [0.79, 1.55] | [−0.86, 1.57] | 9.80 |
| CMB, WL | [0.76, 1.47] | [−0.72, 1.60] | 12.15 |
| CMB, ISW, WL | [0.75, 1.34] | [−0.78, 1.38] | 14.95 |
| CMB, MPK, WL | [0.82, 1.65] | [−0.90, 1.91] | 7.96 |
| CMB, MPK, ISW | [0.76, 1.46] | [−0.89, 1.42] | 11.97 |
| CMB, MPK, ISW, WL | [0.77, 1.56] | [−0.98, 1.57] | 10.06 |

TABLE II: Inferred 95% C.L. constraints for the parameters $\mathcal{G}_{DL}$ or $\Sigma_{\mathtt{MGCAMB};1}$ and $\mathcal{V}_{DL}$ or $\mu_{\mathtt{MGCAMB};1}$ in the second and third parameterizations [73, 82]. These constraints are inferred by using constraints on the parameters $Q_0$, $R_0$, and $D_0$ from the first parameterization [70]. For all of these constraints we set $k_c = \infty$ implying scale independence of the parameterization (10).

… Continued … Latest cosmological data sets show that Dark Energy models (that is the point [1,1] on the plots below) are not ruled out at the 95% confidence limit and so are some modified gravity models.

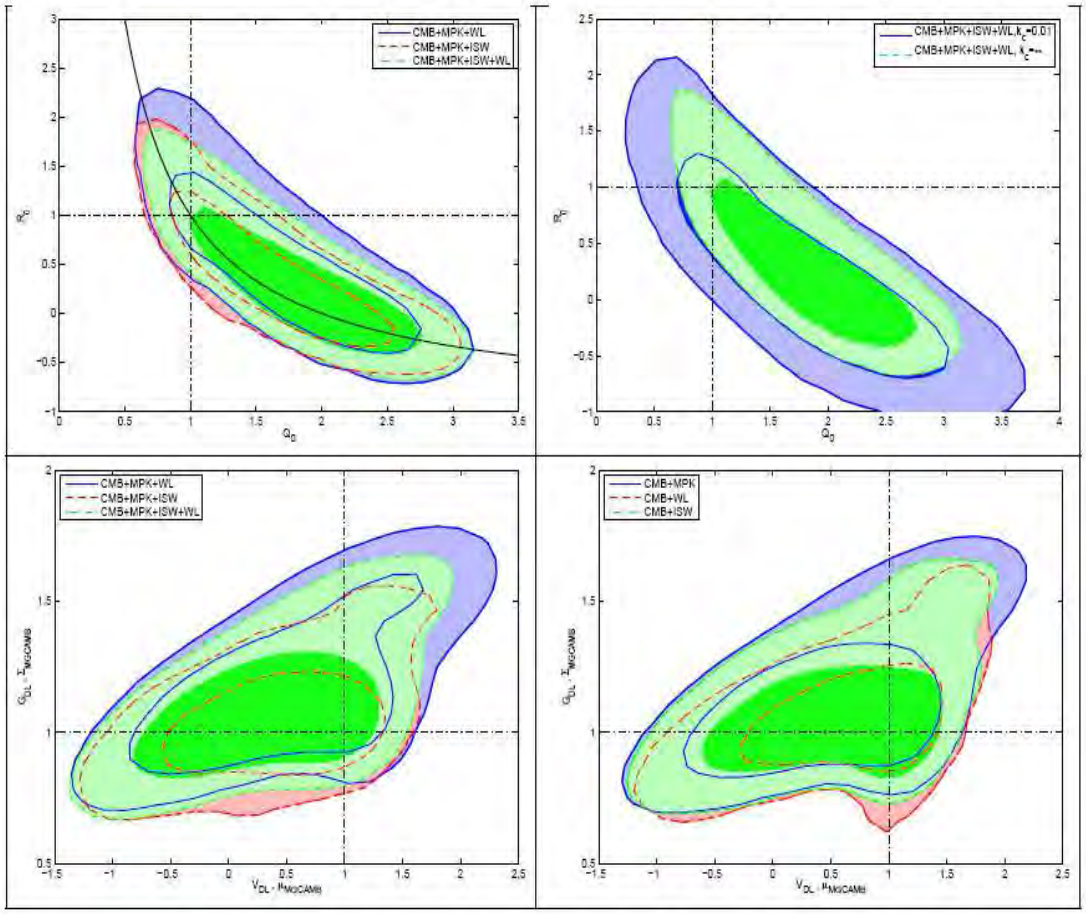


FIG. 1: TOP: 68% and 95% C.L. for the constraints on $Q_0$ and $R_0$. TOP-LEFT: Constraints with $Q$ and $R$ scale-independent ($k_c = \infty$). To show the how the parameter $D_0$ actually represents the degeneracy direction of these parameters, the solid black line is the line $D_0 = 1$. TOP-RIGHT: A comparison of constraints when $Q$ and $R$ are allowed either Scale-dependence ($k_c = 0.01$) or Scale-independence using CMB, ISW, MPK, and WL. Scale-dependent constraints are in red and scale-independent constraints in blue. BOTTOM-LEFT: Inferred 68% and 95% C.L. constraints for the parameters $\mathcal{G}_{DL}$ or $\Sigma_{\texttt{MGCAMB};1}$ and $\mathcal{V}_{DL}$ or $\mu_{\texttt{MGCAMB};1}$ in the second and third parameterizations [73, 82]. These constraints are inferred by using constraints on the parameters $Q_0$, $R_0$, and $D_0$ from the first parameterization [70]. For all of these constraints we set $k_c = \infty$ implying scale independence of the parameterization (10). BOTTOM-RIGHT: We compare inferred constraints on $\mathcal{G}_{DL}$ or $\Sigma_{\texttt{MGCAMB};1}$ and $\mathcal{V}_{DL}$ or $\mu_{\texttt{MGCAMB};1}$ for CMB+MPK (blue) and CMB+WL (red) and CMB+ISW (green) to show the sligt preferences of the datasets. The point $(1, 1)$ indicates the [Dark Energy + GR] values.

## 5) Testing if Cosmic Acceleration is Due to Dark Energy or Modification to Gravity at Cosmological Scales: Implementation and Parameter Correlations

Dossett; Ishak; Moldenhauer. "Testing General Relativity at Cosmological Scales: Implementation and Parameter Correlations". ***Physical Review D*** 84, 123001 (2011).

Abstract: The testing of general relativity plus a Dark Energy component at cosmological scales has become a possible and timely endeavor that is not only motivated by the pressing question of Dark Energy and cosmic acceleration but also by the proposals of some extensions to general relativity that would manifest themselves at large scales of distance. We analyze here correlations between modified gravity growth parameters and some core cosmological parameters using the latest cosmological data sets including the refined Cosmic Evolution Survey 3D weak lensing. We provide parameterized modified growth equations and their evolution. We implement known functional and binning approaches, and propose a new hybrid approach to evolve modified gravity parameters in redshift (time) and scale. The hybrid parameterization combines a binned redshift dependence and a smooth evolution in scale avoiding a jump in the matter power spectrum. The formalism developed to test the consistency of current and future data with general relativity is implemented in a package that we make publicly available and call ISiTGR, an integrated set of modified modules for the publicly available packages CosmoMC and CAMB, including a modified version of the integrated Sachs-Wolfe-galaxy cross correlation module of Ho et al and a new weak-lensing likelihood module for the refined HST-COSMOS weak lensing tomography data. We obtain parameter constraints and correlation coefficients finding that modified gravity parameters are significantly correlated with \sigma_8 and mildly correlated with \Omega_m, for all evolution methods. The degeneracies between \sigma_8 and modified gravity parameters are found to be substantial for the functional form and also for some specific bins in the hybrid and binned methods indicating that these degeneracies will need to be taken into consideration when using future high precision data.

| Correlation coefficients between $\Omega_m$ and $\sigma_8$ and the MG parameters | | | | | | | | |
|---|---|---|---|---|---|---|---|---|
| MG parameters evolved using traditional binning | | | | | | | | |
| Parameter | $Q_1$ | $Q_2$ | $Q_3$ | $Q_4$ | $\mathcal{D}_1$ | $\mathcal{D}_2$ | $\mathcal{D}_3$ | $\mathcal{D}_4$ |
| $\Omega_m$ | 0.0116 | -0.0535 | -0.0338 | -0.0371 | 0.0114 | -0.0988 | 0.0190 | -0.0818 |
| $\sigma_8$ | 0.0937 | 0.1540 | -0.1583 | -0.4267 | 0.2093 | 0.2857 | 0.2377 | 0.0185 |
| MG parameters evolved using hybrid binning | | | | | | | | |
| Parameter | $Q_1$ | $Q_2$ | $Q_3$ | $Q_4$ | $\mathcal{D}_1$ | $\mathcal{D}_2$ | $\mathcal{D}_3$ | $\mathcal{D}_4$ |
| $\Omega_m$ | 0.1571 | -0.1639 | -0.003 | -0.0105 | 0.1814 | -0.2172 | -0.0056 | -0.0070 |
| $\sigma_8$ | 0.1692 | 0.4282 | -0.1076 | 0.1676 | 0.2147 | 0.5390 | 0.1937 | 0.0716 |

| MG parameters evolved using the functional form | | | |
|---|---|---|---|
| Parameter | $Q_0$ | $\mathcal{D}_0$ | $R_0$ |
| $\Omega_m$ | -0.1173 | -0.0294 | 0.0542 |
| $\sigma_8$ | -0.5409 | -0.2631 | 0.5742 |

TABLE I: We list the correlation coefficients for $\Omega_m$ and $\sigma_8$ and the various MG parameters. We see that the MG parameters for all evolution methods are significantly more correlated with $\sigma_8$ than $\Omega_m$, although some correlation with $\Omega_m$ does exist. While traditional binning shows overall the least amount of correlation between the MG parameters and the two cosmological parameters, it, as shown in Fig. 2, has a problematic jump in the matter power spectrum. The hybrid binning is the next least correlated of the methods, with parameters from the functional form evolution showing the most amount of correlation with the two cosmological parameters compared here.

**Continued**

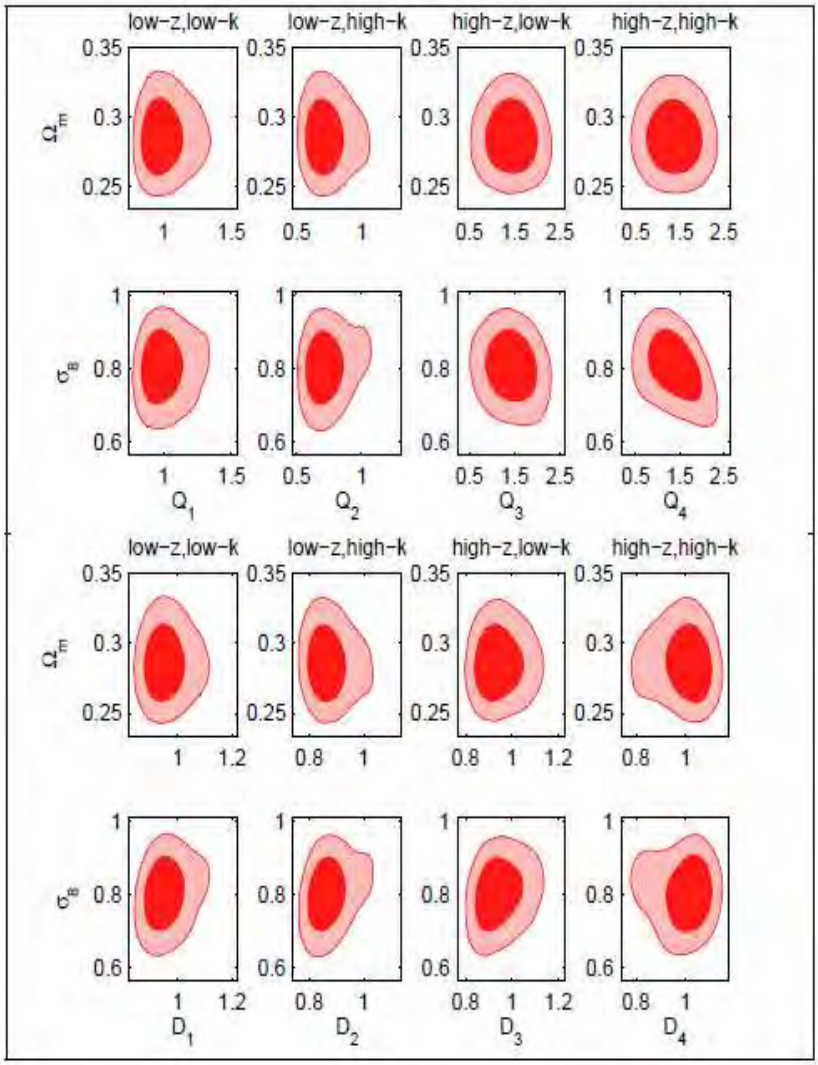


FIG. 6: We plot here the 2D confidence contours for $\Omega_m$ and $\sigma_8$ and the MG parameters $Q_i$ and $\mathcal{D}_i$, $i = 1, 2, 3, 4$ from using traditional bins for $k$ and $z$. As seen in Table I this evolution method has the least amount of correlation between the MG parameters and the two cosmological parameters of the three evolution methods, but as discussed earlier suffers from the appearance of a jump in the matter power spectrum due to the rapid transition between scale bins.

**6) ISiTGR (*Integrated Software in Testing General Relativity*). Software package developed by our theory group to test Dark Energy + general relativity models.** The software is an integrated set of modified modules for the software package CosmoMC for use in testing whether observational data is consistent with general relativity on cosmological scales. It incorporates modifications to the packages: CAMB, CosmoMC, the ISW-galaxy cross correlation likelihood module of Ho et al, and our own weak lensing likelihood module for the refined COSMOS 3D weak lensing tomography of Schrabback et al to test general relativity. It also includes our generalized BAO likelihood module that has recently been incorporated into CosmoMC and uses the recently released WiggleZ BAO data of Blake et al.
Journal-ref: Published in Physical Review D 84, 023012, 2011

**ISiTGR:**
Integrated Software in Testing General Relativity

**Version 1.01**

Developed by Jason Dossett, Mustapha Ishak, and Jacob Moldenhauer.

## What is ISiTGR?

ISiTGR is an integrated set of modified modules for the software package CosmoMC for use in testing whether observational data is consistent with general relativity on cosmological scales. It incorporates modifications to the codes: CAMB, CosmoMC, the ISW-galaxy cross correlation likelihood code of Ho et al, and our own weak lensing likelihood code for the refined COSMOS 3D weak lensing tomography of Schrabback et al to test general relativity. It also includes our generalized BAO likelihood module that has recently been incorporated into CosmoMC and uses the recently released WiggleZ BAO data of Blake et al.

A detailed explanation of the modifications made to these codes allowing one to test general relativity are described in our paper.

## How to get ISiTGR

Two versions of ISiTGR are available. The normal version of ISiTGR uses a functional form to evolve the parameters used to test general relativity and is available here. ISiTGR_BIN, on the other hand, gives you two options to evovle the parameters used to test general relativity. The first option is to bin the parameters in two redshift and two scale bins, alternatively one can use the hybrid evolution method, as seen in our paper, where scale dependence evolves monotonically, but redshift dependence is binned. That code can be downloaded here.

**Downoad Here:** ISiTGR ISiTGR_BIN

ISiTGR for older versions of CosmoMC is available here (**current version is for CosmoMC 10/2011**).

## Running ISiTGR. (ReadMe)

To run ISiTGR you must first download and install CosmoMC (October 2011 version). You can find download instructions, system requirements, and setup instructions for CosmoMC in the CosmoMC ReadMe. Then, simply copy the contents of the unzipped ISiTGR folder to the CosmoMC folder, edit the Makefile for your compilers, compile (extra compiling step here), and you are ready to go. Detailed explanations of the specific options available in each of the ISiTGR codes are availalble in the ISiTGR ReadMe.

**PRODUCTS:**

## a) Publications in Refereed Journals:

1) Title: Constraints on growth index parameters from current and future data
Authors: Jason Dossett (UTDallas), Mustapha Ishak (UTDallas), Jacob Moldenhauer (UTDallas), Yungui Gong, Anzhong Wang
Journal-ref: Journal of Cosmology and Astroparticle Physics 1004:022, 2010.

2) Contiguous redshift parameterizations of the growth index
Authors:Mustapha Ishak, Jason Dossett (The University of Texas at Dallas)
Journal-ref: Phys.Rev.D80:043004,2009

3) Growth factor parametrization in curved space
Authors:Yungui Gong, Mustapha Ishak, Anzhong Wang
Journal-ref: Phys.Rev.D80:023002,2009

4) Title: Supernova, baryon acoustic oscillations, and CMB surface distance constraints on f(G) higher order gravity models (as an alternative to Dark Energy)
Authors: Jacob Moldenhauer (UTDallas), Mustapha Ishak (UTDallas), John Thompson (UTDallas), Damien A. Easson (UTDallas)
Journal-ref: Physical Review D. 81:063514, 2010.

5) Title: Figures of merit and constraints from testing General Relativity using the latest cosmological data sets including refined COSMOS 3D weak lensing
Authors: Jason Dossett, Jacob Moldenhauer, Mustapha Ishak
Journal-ref: Published in Physical Review D 84, 023012, 2011

6) Title: Testing General Relativity at Cosmological Scales: Implementation and Parameter Correlations
Authors: Jason Dossett, Mustapha Ishak, Jacob Moldenhauer
Journal-ref: Published in Physical Review D 84, 123001, 2011

7) Title: The growth of structure in the Szekeres inhomogeneous cosmological models and the matter-dominated era
Authors:Mustapha Ishak, Austin Peel (The University of Texas at Dallas)
Journal-ref: Phys. Rev. D85, 083502, 2012

8) Title: Large-scale growth evolution in the Szekeres inhomogeneous cosmological models with comparison to growth data
Authors:Austin Peel, Mustapha Ishak, M. A. Troxel (The University of Texas at Dallas)
Journal-ref: Phys.Rev.D86,123508,2012

9) Spatial curvature and cosmological tests of general relativity
Authors:Jason Dossett, Mustapha Ishak (The University of Texas at Dallas)
Journal-ref: Phys. Rev. D86, 103008, 2012

**Invited Talks, Colloquia, Seminars and presentations at conferences:**

**PI, Ishak-Boushaki**

1. Conference of the American Astronomical Society, AAS Meeting #215, Washington DC, 2010. On The Growth Rate Index Parameter and Cosmic Acceleration.

2. Colloquium at the Louisiana State University, Baton Rouge, LO, 2010.
   Why is the expansion of the universe accelerating?

3. Colloquium at the University of New Mexico at Socorro, NM, 2010.
   Why is the expansion of the universe accelerating?

4. Colloquium at the University of Texas at Brownsville, Brownsville, TX, 2010.
   Why is the expansion of the universe accelerating? One of the biggest puzzles in cosmology!

5. Public Lecture to the Texas Astronomy Society, University of Texas at Dallas, Richardson, TX, 2010. Why is the expansion of the universe accelerating?

6. Colloquium at the University of Texas at Arlington, Arlington, TX, 2010.
   Why is the expansion of the universe accelerating? One of the biggest puzzles in cosmology!
7. Invited Colloquium at Baylor University, "Why is cosmic expansion accelerating?" (Baylor, TX,2011)

8. Invited plenary talk On Cosmic Acceleration at the Joint Fall 2011 Meeting of the Texas Sections of the APS, AAPT, and Zone 13 of the SPS, Volume 56, Number 7, (Commerce, TX, 2011)

9. Invited Colloquium at University of Oklahoma, "Why is cosmic expansion accelerating?" (Norman, OK, 2011)

10. Invited plenary session talk on Cosmic Acceleration at the 8$^{th}$ International Conference on Theoretical Physics at University of Constantine, (Constantine, 2011).

11. Invited parallel talk on Inhomogeneous models and Cosmic Acceleration at the 8$^{th}$ International Conference on Theoretical Physics at University of Constantine, (Constantine, 2011).

12. Apparent Acceleration Due to Relativistic Cosmological Models More Complex Than FLRW as a Possible Alternative to Dark Energy
    Ishak, Mustapha; Richardson, James; Whittington, Delilah; Nwankwo, Anthony; Sussman, Roberto
    Proceedings of the Twelfth Marcel Grossmann Meeting on General Relativity in Paris, France, edited by Thibault Damour, Robert T. Jantzen and Remo Ruffini. ISBN 978-981-4374-51-4. Singapore: World Scientific, 2012, p.1359.

13. Competing explanations for cosmic acceleration or why is the expansion of the universe is accelerating? Ishak, Mustapha.
AIP Conference Proceedings of the 8th International Conference on Progress in Theoretical Physics. Volume 1444, pp. 66-76 (2012). (c) 2012: American Institute of Physics.

14. New Results from Using Inhomogeneous Cosmological Models in an Era of Precision Cosmology Observations. Ishak, Mustapha B.; Nwankwo, A.; Peel, A.
Bulletin of the American Astronomical Society meeting #219, #312.03. 01/2012. Austin, Texas. (c) 2012: American Astronomical Society.

15. Colloquium at the University of Texas at San Antonio, "Why is the expansion of the universe accelerating?" (UTSA San Antonio, TX, 2012

16. Invited Presentation at the NSM Advisory Council meeting, 'The UTD Cosmology Research Efforts in Understanding the Problems of Dark matter and Dark Energy." (Nov. 2012)

**Graduate Student Jacob Moldenhauer:**

1. Seminar at CASPER(Center for Astrophysics, Space Physics and Engineering Research) series of talks 2010, Baylor University, Waco, Texas, March 26, 2010. "Dynamics and Phenomenology of Higher Order Gravity Cosmological Models"

**2.** Poster Presented at 215th American Astronomical Society Meeting
Washington, D.C., January 3-7, 2010. "Dynamics and Phenomenology of Higher Order Gravity Cosmological Models"

**3.** Poster presented at Berkeley Center for Cosmological Physics, Essential Cosmology for the Next Generation: Playa del Carmen, Mexico, January 11-15, 2010. "Dynamics and Phenomenology of Higher Order Gravity Cosmological Models"

4. Testing extensions of General Relativity using the latest cosmological data sets
Moldenhauer, Jacob; Dossett, Jason; Ishak, Mustapha
Bulletin of the American Physical Society, APS April Meeting 2012, March 31-Apr 3, 2012, abstract #K1.082.

**Graduate student Jason Dossett:**

1. Poster Presented at 217th American Astronomical Society Meeting, Seattle, Washington, January 9-13, 2011. "New Results on Testing Modified Gravity versus Dark Energy From the Latest Combined Cosmological Data Sets."

2. Poster Presented by Jason Dossett at 217th American Astronomical Society Meeting, Seattle, Washington, January 9-13, 2011. "New Results on Testing Modified Gravity

versus Dark Energy From the Latest Combined Cosmological Data Sets."

3. Talk by Jason Dossett at the 2011 Fall Meeting of the Texas Section of the APS Commerce, TX, October 6-8, 2011. A Figure of Merit Analysis of Current Constraints on Testing General Relativity using the Latest Cosmological Data Sets

4. ISiTGR: A Software Package for Testing General Relativity at Cosmological Scales.
   Dossett, Jason; Ishak, M.; Moldenhauer, J
   Bulletin of the American Astronomical Society, AAS Meeting #219, #112.06. 01/2012.
   (c) 2012: American Astronomical Society.

5. Correlations Between Cosmological Parameters and Modified Gravity Parameters when Testing Gravity at Cosmological Scales
   Dossett, Jason; Ishak, Mustapha; Moldenhauer, Jacob
   Bulletin of the American Physical Society, APS April Meeting 2012, March 31-Apr 3, 2012, abstract #L6.005.

## b) Web site or other Internet sites that reflect the results of this project;

**ISiTGR** (***Integrated Software in Testing General Relativity***). **Software package developed by our theory group to test Dark Energy + general relativity models.** The software is an integrated set of modified modules for the software package CosmoMC for use in testing whether observational data is consistent with general relativity on cosmological scales.

Journal-ref: Published in Physical Review D 84, 023012, 2011

Available online at: http://www.utdallas.edu/~jnd041000/isitgr/